



Published in final edited form as:

J Nucl Med. 2014 December ; 55(12): 2003–2011. doi:10.2967/jnumed.114.141416.

Multimodality Imaging of Alzheimer Disease and Other Neurodegenerative Dementias

Ilya M. Nasrallah¹ and David A. Wolk²

¹Department of Radiology, Hospital of the University of Pennsylvania, University of Pennsylvania, Philadelphia, Pennsylvania

²Department of Neurology, Hospital of the University of Pennsylvania, University of Pennsylvania, Philadelphia, Pennsylvania

Abstract

Neurodegenerative diseases, such as Alzheimer's disease, result in cognitive decline and dementia and are a leading cause of mortality in the growing elderly population. These progressive diseases typically have insidious onset, with overlapping clinical features early in disease course that makes diagnosis challenging. Neurodegenerative diseases are associated with characteristic, although not completely understood, changes in the brain: abnormal protein deposition, synaptic dysfunction, neuronal injury and neuronal death. Neuroimaging biomarkers – principally regional atrophy on structural MRI, patterns of hypometabolism on ¹⁸F-fluorodeoxyglucose (FDG) PET, and detection of cerebral amyloid plaque on amyloid PET – are able to evaluate the patterns of these abnormalities in the brain to assist and improve early diagnosis of these conditions as well as to help predict disease course in the future. There are unique strengths of these techniques as well as synergies in multimodality evaluation of the patient with cognitive decline or dementia. This review will discuss the key imaging biomarkers from MRI, ¹⁸F-FDG PET, and amyloid PET, the imaging features of the most common neurodegenerative dementias, the role of various neuroimaging studies in differential diagnosis and prognosis, and introduce some promising imaging techniques currently under development.

Introduction

Neurodegenerative diseases cause progressive cognitive decline and, ultimately, dementia affecting a growing number of people with the increasing elderly population. Alzheimer's disease (AD) is the leading cause of neurodegenerative dementia, followed by dementia with Lewy bodies (DLB), frontotemporal lobar degeneration (FTLD), and even rarer syndromes of progressive supranuclear palsy (PSP) and corticobasal degeneration (CBD). These syndromes are caused by a progressive neuronal dysfunction and loss, which result in characteristic symptoms and features in mid to late disease course, but overlap in cognitive and behavioral profiles can make them difficult to distinguish clinically at presentation. This review will introduce clinical aspects of neurodegenerative dementia, provide an overview

of imaging modalities, review the imaging features of specific neurodegenerative dementias, discuss the use of imaging biomarkers for differential diagnosis and prognosis, and touch upon future directions for imaging in neurodegenerative dementia. Selected appropriately, multimodality imaging with MRI and PET has the potential to improve diagnosis and management of patients with neurodegenerative dementia.

Although no definitive disease-modifying therapies are yet available, appropriate and early diagnosis allows selection of interventions and symptomatic treatments most likely to provide benefit and avoidance of therapies that are not likely to help, but with potential to cause side effects. Furthermore, it allows life planning for patients before that capacity is lost and preparation for caretakers. While current therapies offer modest symptomatic benefit and may delay institutionalization, there are considerable ongoing efforts towards novel treatments; such therapies would likely be most efficacious if started early in the disease course before significant neurodegeneration occurs. Current benefits of early diagnosis are modest and difficult to quantify, leaving controversy over whether early screening should be performed(1).

Even in affluent countries, it is estimated that at least half of dementia cases are undiagnosed(2). Diagnosis of neurodegenerative dementia is even more challenging at earlier stages where symptoms are subtle and the characteristic syndromic features may be incompletely manifest. Compensatory mechanisms, termed 'cognitive reserve', which vary between individuals depending on multiple factors including level of education, and patient comorbidities such as coexisting depression may mask initial cognitive effects of neurodegeneration. Additionally, there is heterogeneity in the clinical phenotype of neurodegenerative condition that may obfuscate diagnosis. Most prominently, AD is associated with several 'atypical' presentations that are relatively common, particularly in early onset dementia (prior to age 65). For example, a primary progressive aphasia (PPA) variant of AD presents with language difficulties instead of the more typical amnesia(3), and, thus, is often confused with PPA due to FTL spectrum neurodegeneration.

Neuroimaging biomarkers may assist in the diagnosis of neurodegenerative dementia and may provide prognostic information. Structural MRI, ^{18}F -FDG PET, and, more recently, amyloid PET may be useful adjuncts to clinical examination; novel MRI techniques and new PET radiotracers under development may further expand our diagnostic ability. These and other biomarkers of dementia can be classified into two groups: those that evaluate underlying molecular pathology, such as amyloid PET, and those that evaluate for evidence of neurodegeneration, including structural MRI and ^{18}F -FDG PET. Perfusion SPECT is also used to evaluate for regional perfusion abnormalities; patterns tend to match those for ^{18}F -FDG PET but SPECT has technical disadvantages and poorer accuracy than ^{18}F -FDG PET (4) and is not discussed further in this review. As is the case for all diseases of the elderly, evaluation of biomarkers must be considered in the setting of the normal volume, neural, and synaptic losses of aging. This parallels considerations for standard psychometric testing also used for evaluation of cognitive decline, the results of which depend upon language, education, and culture. Comparison to age- and gender-matched normative standards are important for the imaging specialist visually interpreting these studies and, particularly when quantifying data from imaging tests(5).

Structural MRI is a mainstay of evaluation of patients with cognitive deficits to help exclude non-neurodegenerative etiologies such as vascular disease. Further, structural MRI can show evidence of focal atrophy to suggest specific neurodegenerative diseases. While some atrophy patterns are clear in advanced stages, quantitative post-processing techniques may assist in early diagnosis of neurodegenerative dementias based on regional gray matter volume and thickness. Limitations of MRI include contraindications in patients with pacemakers and other implanted devices and study degradation by patient motion.

PET is used to evaluate a growing number of molecular targets in the brain. Clinical PET, however, is limited to evaluation of cerebral metabolism using ^{18}F -FDG and newer amyloid imaging agents. Distribution of FDG in the brain depends upon regional metabolism and blood flow, which change in response to synaptic activity and cell density. Both of these are affected in neurodegenerative dementias, with regional differences allowing for discrimination of the underlying etiology. Sensitivity to synaptic activity can also be a limitation of ^{18}F -FDG PET, as centrally-active medications and comorbid psychiatric illness, such as depression, can change or obscure patterns from underlying neurodegeneration(6).

Amyloid PET evaluates for the presence of fibrillar β -amyloid deposits, one of the hallmark pathologic substrates of AD. Three amyloid radiotracers are approved by the United States Food and Drug Administration for clinical use: ^{18}F -florbetaben, ^{18}F -florbetapir, and ^{18}F -flutemetamol, although most studies of amyloid PET used the first agent developed, ^{11}C -Pittsburgh Compound B(7). While there are some differences, these agents appear to provide similar performance for the detection of cerebral amyloid(8). Amyloid PET shows detectable cortical uptake with high sensitivity and specificity when a moderate to severe burden of plaque is present(9). Clinically, amyloid PET is interpreted dichotomously as positive, indicating presence of cortical amyloid, or negative. Limitations of amyloid PET include prominent non-specific white matter uptake for clinically available radiotracers, making visual evaluation more difficult. Furthermore, cortical amyloid is not specific for the presence of cognitive symptoms, affecting positive predictive value. Beyond amyloid, there are numerous other pathologic proteins of interest for neurodegenerative diseases, including tau and alpha-synuclein, which are targets for tracer development(10).

Medical images have traditionally been interpreted visually by imaging specialists and referring clinicians. In order to better quantify this data, several visual ratings scales have been developed. However, many of the changes seen in neurodegeneration are difficult or impossible to evaluate by the human eye and high inter-rater reliability can be difficult to achieve with visual rating scales. Much research has used manual delineation of regions of interest or semi- or fully-automated computational tools for data extraction and quantification, such as voxel-based morphometry. These methods allow for global and regional quantification of brain volume or cortical thickness for MRI and of radiotracer distribution and kinetics for PET. Computational methods can generate and evaluate numerous regions of interest, and some groups have attempted to reduce this complexity to summative scores(11, 12). Many studies have shown superiority of more quantitative approaches(13, 14). While powerful, many computational approaches are not fully standardized and can be difficult to implement, let alone validate, at other institutions.

Normal aging

Cerebral volume loss is typical during normal aging. These changes include global cerebral as well as more regional volume loss (Figure 1), particularly involving the prefrontal cortex(15). Hippocampal atrophy rates are also higher than global atrophy rates in cognitively normal individuals and increase with age(15, 16). Normally, gray matter shows high uptake of glucose; there are mild regional decreases with aging(11) that do not match typical patterns associated with neurodegeneration. Amyloid PET has high sensitivity for cerebral amyloid plaque, and is often negative in cognitively normal individuals. However, it is well established that cognitively normal individuals can have detectable cerebral amyloid deposition. The prevalence of cerebral amyloid increases from 10–15% at age 65 to about 50% at age 85(17). This uptake in cognitively normal individuals is thought to reflect preclinical AD(18).

Alzheimer's disease

AD is usually characterized primarily by memory dysfunction with insidious onset and a long preclinical phase. While pathologic evaluation for the presence of β -amyloid neuritic plaques and tau-protein containing neurofibrillary tangles is required for definitive diagnosis, recent diagnostic criteria have identified biomarkers that can increase confidence in the diagnosis of underlying AD(19). Interest in early diagnosis has identified two pre-dementia groups. A prodromal stage is clinically synonymous to mild cognitive impairment (MCI), defined by the presence of objective cognitive impairment without significant functional decline (20). However, it is a heterogeneous group and many MCI patients – sometimes the majority depending on method of classification – do not have underlying AD. Recent criteria use the presence of biomarker evidence of amyloid pathology and neurodegeneration to increase the confidence the MCI represents prodromal AD(20). The presence of a 'preclinical' stage of AD has also been defined as including those with no objective cognitive deficit or biomarker evidence of neurodegeneration but with evidence of cerebral amyloid deposition(21); note that these criteria were developed for research purposes, with the hope that defining this group could lead to future preventative or disease modifying treatments at this stage.

The hallmark MRI biomarker for AD, and by far the most studied in all of neurodegeneration, is hippocampal atrophy (Figure 2). Average hippocampal volume reduction is 20–25% in AD and 10–15% in MCI(22). Visual assessment for pathologic hippocampal atrophy at early stages is challenging, particularly in MCI, resulting in lower sensitivity for AD. Automated methods for hippocampal evaluation have been developed but are not widely available(23). The lack of standardized methodology for measurement of hippocampal volumes has limited incorporation of this biomarker into clinical practice. Computational evaluation of the entire brain for evidence of focal volume or cortical thickness reductions show other characteristic regions affected in AD, such as the precuneus and lateral parietal lobes; these AD signature patterns correlate with severity of cognitive decline(12, 24).

¹⁸F-FDG PET shows characteristic hypometabolism in the hippocampi/medial temporal lobes, posterior cingulate, precuneus, and lateral temporoparietal cortex, with the most reliable early changes seen in the posterior cingulate cortex(25, 26) (Figure 2). Milder but similar regional changes are seen in MCI likely to progress to clinical AD, (5), while more advanced AD typically shows frontal lobe involvement. It has long been held that metabolism may become abnormal earlier in the course of AD than MRI measures(27), but some recent evidence suggests that these neurodegenerative biomarkers may change simultaneously(28). In typical amnesic AD, hypometabolism is usually bilateral, but may be asymmetric(29), and spares the basal ganglia, somatosensory cortex, and occipital cortex(26, 30). ¹⁸F-FDG PET can discriminate AD patients from healthy controls with high sensitivity and specificity(11). Use of ¹⁸F-FDG PET has been shown to improve accuracy in diagnosis of AD compared to clinical evaluation(31) and to change diagnosis in about a quarter of patients(32). Amyloid PET is positive with high sensitivity for AD in series with pathologic confirmation(33). Approximately 50% of MCI patients show positive amyloid scans, particularly those with deficits in multiple cognitive domains(34). Cerebral amyloid accumulation appears to start decades before onset of dementia(35) and may be the earliest biomarker to show measurable abnormality(28).

There are several uncommon, atypical presentations of AD. These consist of the logopenic variant of primary progressive aphasia (lvPPA), marked by a primary impairment in language, posterior cortical atrophy (PCA), primarily associated with visuospatial impairment, and frontal variant AD, characterized by behavioral and executive function change(36, 37). These atypical forms represent about one third of young onset AD and at least 5% of late-onset AD cases and pose diagnostic challenges(36). Neuroimaging demonstrates distinct anatomic distribution of gray matter atrophy and hypometabolism consistent with the clinical presentations of these conditions. LvPPA tends to display greater left peri-Sylvian/temporoparietal decreases and PCA is associated with parietal-occipital decreases(38). The pattern of amyloid deposition seen at autopsy and on amyloid PET in these atypical presentations is not clearly distinct from typical AD(39).

Frontotemporal Lobar Degeneration

FTLD is a heterogeneous group of neurodegenerative conditions that share clinical features and pathologic and genetic etiologies. The behavioral variant (bvFTD) is the most common subtype, clinically characterized by early personality and behavior changes, semantic dementia (SD) and progressive nonfluent aphasia (PNFA), demonstrate primary language changes, and there are overlap syndromes with mixed features. Age of onset is typically younger than AD, generally before age 65. FTLD can be associated with abnormal aggregates of various proteins, including primarily tau-based pathology, transactive response DNA Binding Protein-43 (TDP-43) or fused in sarcoma (FUS)(3).

MRI demonstrates frontal and anterior temporal atrophy, which can be severe resulting in “knife blade gyri” appearance. Subtypes of FTLD differ in atrophy patterns (Figure 3). BvFTD shows greatest atrophy in the anterior frontal lobes, SD typically involves the anterior temporal lobes, and PNFA the left anterior perisylvian region, particularly left ventrolateral prefrontal cortex. Asymmetry is common, particularly in language variants

where the left side is more severely affected(40). Regional atrophy patterns have been used to distinguish these three subtypes of FTLN with high sensitivity and specificity(41). There is some evidence that atrophy patterns may relate to underlying pathologic subtype(42). However, this link is probabilistic at best: on an individual level, each atrophy pattern can be seen in the setting of multiple clinical subtypes of FTLN-spectrum pathologies. There are corresponding patterns seen on ^{18}F -FDG PET (Figure 3). BvFTD shows predominately frontal hypometabolism, with varying involvement of the anterior cingulate cortex and anterior temporal lobes(43). SD is associated with predominately anterior temporal lobe hypometabolism that is usually asymmetric(44), while PNFA shows prominently asymmetric left anterior perisylvian hypometabolism(45). Rarely, FTLN can present with an AD pattern of hypometabolism, although usually associated with frontal hypometabolism(5). Additionally, amyloid PET is expected to be negative in FTLN, but a significant minority of patients have positive scans, with rates differing depending on FTLN subtype; it is thought that these cases represent comorbid AD pathology or, more likely, misdiagnosis of the underlying etiology (46, 47).

There are several less common neurodegenerative etiologies of dementia, including PSP and CBD, which have been classified both as within the FTLN-spectrum and as atypical Parkinsonian syndromes given their association with characteristic motor symptoms. PSP is characterized by oculomotor abnormality and gait instability, with less frequent executive function, visuospatial, and language impairments. MRI shows profound midbrain atrophy resulting in what has been termed the ‘hummingbird’ appearance of the brainstem as well as pontine, thalamic, striatal and milder frontal cortical atrophy. Superior cerebellar peduncle atrophy is characteristic (Figure 4). ^{18}F -FDG PET may show symmetric prefrontal and primary/supplemental motor cortex hypometabolism, also with deep nuclear and midbrain hypometabolism(30). CBD is often associated with a clinical constellation of findings termed corticobasal syndrome (CBS) which includes asymmetric parkinsonism, apraxia, gait disturbance, and alien hand phenomenon. In CBD, there is asymmetric frontoparietal atrophy involving paracentral and parasagittal structures(48) (Figure 4). ^{18}F -FDG PET shows asymmetric, often unilateral hypometabolism, seen contralateral to predominant motor symptoms, involving parietotemporal, sensorimotor cortex, prefrontal cortex, caudate, and thalamus; asymmetry and sensorimotor cortex involvement are relatively unique(30). It is worth noting that CBS lacks specificity with regard to underlying pathology, as it can be seen with other FTLN-associated, as well as AD, pathology. Conversely, typical CBD pathology can present with syndromes similar to PSP and PNFA, amongst others(49).

Dementia with Lewy Bodies

DLB is the second most common form of neurodegenerative dementia. Pathologically similar to Parkinson’s disease, with alpha-synuclein-containing Lewy bodies on pathology, DLB is clinically distinguished from Parkinson’s disease dementia (PDD) by presentation of dementia before or within one year of onset of Parkinsonian movement symptoms(50). At least 70–80% of DLB patients have cerebral amyloid plaque(51) with many cases meeting pathologic criteria for mixed DLB/AD. The core clinical features of DLB are parkinsonism, cognitive fluctuations and visual hallucinations. Cognitive and behavior features include

abnormalities of executive function, attention, and visuospatial ability, hallucinations, depression, and anxiety(50).

Structural MRI results have been variable, with cortical atrophy probably due to associated AD pathology, as studies show that subjects with DLB but no AD pathology have brain volumes similar to healthy controls, including volumes of medial temporal structures(52). ¹⁸F-FDG PET shows occipital hypometabolism in addition to involvement of regions affected by AD: posterior cingulate, temporoparietal cortex, and, less prominently, frontal cortex, although medial temporal metabolism is generally preserved(30, 53) (Figure 5). Greater hypometabolism is correlated with worse severity of dementia(53). Amyloid PET is usually positive in DLB, while usually negative in PDD(51). Unlike other neurodegenerative dementias, DLB shows abnormally decreased tracer uptake in the striatum on PET and SPECT imaging of the dopaminergic system, with ¹²³I-FP-ioflupane (GE Healthcare) the most widely used(54).

Differential diagnosis of dementia

In addition to sometimes overlapping clinical presentation, various etiologies of neurodegenerative dementia can have similar appearance with a variety of imaging modalities. Most imaging studies have focused on distinction from healthy control groups, however differential diagnosis has also been investigated, with studies generally showing improvement in diagnosis compared to clinical evaluation. While studies showing high accuracy using biomarkers to differentiate between typical patients and healthy controls demonstrate important features of disease, the most relevant studies to clinical evaluation will interrogate the performance of the biomarkers earlier in the disease course and in less typical presentations where clinical assessment has poorer performance; these studies are however difficult to perform largely due to challenges of confirming true diagnoses. Thus, although many measures have shown strong ability to distinguish between groups in controlled studies, the utility in evaluation of individual patients will be lower due to overlaps in biomarker results in these more challenging cases.

MRI has a central role in the differential diagnosis of dementia. It is primarily used to exclude non-neurodegenerative etiologies of dementia (Figure 6). Vascular dementia, or vascular cognitive impairment, is arguably the second most common etiology of dementia and is typically associated with severe small vessel ischemic change and lacunar infarcts, although large territory infarcts can also present with dementia. Normal pressure hydrocephalus may be suggested based upon ventricular enlargement although imaging is far from definitive in this population. Sporadic Creutzfeldt-Jakob Disease, a prion disease, is often characterized by cortical, basal ganglia and medial thalamic diffusion restriction, frequently with associated FLAIR abnormalities. Other conditions, including paraneoplastic, infectious, and inflammatory conditions can cause cognitive decline and may be identified on MRI. Beyond excluding alternative etiologies, MRI has utility in distinguishing etiologies of neurodegenerative disease: studies using automated image analysis software have found that MRI can be used to distinguish AD and FTLN(55) as well as distinguishing subtypes of FTLN(56). Preservation of hippocampal and lateral temporoparietal volumes favors DLB over AD(52).

Multiple studies have shown that ^{18}F -FDG PET is useful in the differential diagnosis of dementia, although few have compared performance in more than two neurodegenerative conditions and most have used clinical diagnosis as the reference standard, limiting generalizability. Normal ^{18}F -FDG uptake significantly reduces the likelihood of an underlying neurodegenerative process(31). ^{18}F -FDG PET shows high sensitivity and specificity to distinguish AD from FTLN(13). The presence of occipital hypometabolism can distinguish DLB from AD, which are otherwise similar, with 85–90% sensitivity and 80–90% specificity(57). Vascular dementia can also be differentiated from AD by ^{18}F -FDG PET, showing focal asymmetric hypometabolism with more common involvement of the deep nuclei(58). The few studies that have studied mixed cohorts have shown high performance in differential diagnosis(59), with estimated 87% sensitivity(60) and 81% specificity to distinguish AD from other causes of dementia(6). Panegyres *et al.* showed 78% sensitivity and 81% specificity for detection of AD versus other conditions included in the study: FTLN, DLB, PPA, and depression. Specificity was >95% for diagnosis of the other etiologies, however sample sizes were small. Topography on PET generally shows strong correlation with clinical syndrome, but may be less accurate in distinguishing the underlying pathology, such as in some subtypes of PPA in which several different pathologies can present with similar clinical syndromes and patterns of neurodegeneration(61). Multiple studies have shown improved accuracy, improved diagnostic confidence, and lower inter-rater variability over clinical evaluation of neurodegenerative dementia alone(13, 31).

Amyloid PET has proven utility in the differential diagnosis of neurodegenerative dementia. Amyloid PET can identify patients likely to have AD or DLB versus other causes of dementia(46). This utility is highest in cases of early onset dementia, where AD and FTLN each account for almost half of cases. Amyloid PET and ^{18}F -FDG PET have similar accuracy in distinguishing these diagnoses, with amyloid PET showing higher sensitivity (47). Amyloid PET can also be used to distinguish non-amnesic presentations of AD from FTLN and amnesic presentations of FTLN from typical AD. Primary progressive aphasia, for example, can be associated with either AD or FTLN pathology. Amyloid PET may also be useful to evaluate for the presence of AD pathology in patients with neurologic and psychiatric comorbidities, which may interfere with both neurocognitive testing and alter the metabolic pattern of ^{18}F -FDG PET, but should not affect amyloid PET. Vascular dementia is an important differential diagnosis for AD with distinct therapeutic options, however patients with severe small vessel ischemic changes of the white matter or multiple infarcts evident on MRI may have atypical findings on MRI or ^{18}F -FDG PET. Amyloid PET is not useful in distinguishing AD from DLB(46).

Imaging biomarkers for prognosis

Biomarkers have been extensively evaluated for efficacy in determining progression of cognitive decline. These include neurocognitive test results, genetic tests, vascular risk factors, and CSF sampling, in addition to imaging biomarkers(62); this review focuses on imaging biomarkers. There are several limitations in the application of biomarker studies to clinical use. First, the patient population included in a research study is very likely to differ from that of any particular clinical setting, which can have an effect on biomarker

utility(63). Second, it is important to note that proven utility of a biomarker in one phase of disease does not indicate that it would be able to inform on prognosis at another stage, as biomarkers appear to have a characteristic dynamic period(28). Furthermore, while many studies derive methods for biomarker utilization, these need to be validated and standardized in independent, larger samples.

Numerous studies have evaluated associations between brain structural measurements on MRI and progression of cognitive decline and onset of dementia. Cross-sectional medial temporal lobe and hippocampal volume and longitudinal measures of rate of atrophy are sensitive and predictive structural features for future decline. Worsening MTL atrophy is associated with greater progression to AD both for cognitively normal individuals and MCI(64). Global atrophy is also a risk factor. Patients with atrophy on MRI at the time of diagnosis of MCI have demonstrated greater rates of conversion to AD within 3–5 years than those without atrophy(65). Similarly, progressors to AD amongst MCI and normal individuals have higher rates of ventricular enlargement than those that remain stable (65, 66). Unfortunately, hippocampal atrophy is not specific to AD; for example, it is frequently observed in some types of FTLD. Associations between atrophy and progression have been shown in other neurodegenerative dementias. Frontal atrophy in patients with FTLD had greater rates of cognitive decline than temporal variants(67). Atrophy rates in DLB correlated with worsening cognitive decline(68). However, while sensitive in group analyses, there is overlap between groups for structural MRI measures, including hippocampal volume in AD, which may limit the usefulness for prognosis in individual patients(65).

¹⁸F-FDG PET has also been shown to provide important prognostic information for progression of cognitive decline. ¹⁸F-FDG PET shows high specificity; negative ¹⁸F-FDG PET indicates progression from MCI to dementia is unlikely(5, 6). Hypometabolism in AD-characteristic regions, including posterior cingulate, lateral temporoparietal lobes, and medial temporal lobes is predictive of conversion from MCI to dementia(29). Declining hypometabolism in MCI and AD is associated with greater cognitive and functional decline(29). Use of ¹⁸F-FDG PET for prognosis of other forms of neurodegenerative dementia has been studied much less. In one small study, non-demented individuals who showed occipital hypometabolism were at increased risk for conversion to DLB, especially if temporoparietal hypometabolism was also present(69). ¹⁸F-FDG PET also appears to predict neurodegeneration in carriers of a mutation associated with FTLD prior to symptom onset(70).

The presence of cerebral amyloid deposition has prognostic information for cognitively normal individuals and MCI. Most studies of cerebral amyloid have shown relative stability in demented patients, suggesting that changes in amyloid burden is not likely to provide clinically useful information at this stage in the absence of a treatment intervention that modulates amyloid deposition(26). Cerebral amyloid can be detected years, even decades, before onset of cognitive decline(35). Cognitively intact patients with positive amyloid PET have been reported in some, but not all, studies to display poorer performance on cognitive testing(71). There is also an association between amyloid positivity and higher hippocampal atrophy rates in healthy and MCI individuals(16). Finally, MCI and normal individuals with

amyloid have higher rates of conversion to AD and MCI, respectively(35, 72). However, it remains uncertain whether all cognitively normal individuals with a positive amyloid scan will progress to dementia. The predictive value with regard to the timing of cognitive decline is also unclear, with many individuals not displaying decline after > 5 years from a positive study(73). Nonetheless, the study of amyloid positive, cognitively normal individuals is a major focus of research in the field.

Fewer studies have been performed to compare the relative efficacy and contribution of different biomarkers for estimation of prognosis in neurodegenerative dementia. Imaging biomarkers in many cases show improved predictive ability compared to clinical evaluation/ neurocognitive testing(74), although this is not uniform. Several studies have shown slightly higher predictive ability for ^{18}F -FDG PET compared to structural MRI in separating MCI from normal controls and in determining progression from MCI to AD(74), with a smaller number of studies showing similar performance(75). Rowe *et al.* have shown that amyloid PET positivity is a stronger predictor of progression of cognitively normal to MCI and from MCI to AD than hippocampal volume, with high positive predictive value(72). One study comparing amyloid PET and ^{18}F -FDG PET for conversion of MCI to AD showed higher sensitivity for amyloid PET, higher specificity for ^{18}F -FDG PET, and similar accuracy(14). Prestia *et al.* evaluated multiple biomarkers in two different cohorts, and showed that amyloid measures had the highest sensitivity for progression to AD and hippocampal volumes the highest specificity to exclude stable MCI, with ^{18}F -FDG PET showing intermediate values for both(63).

Combining biomarker data can improve prognostic ability. Adding cognitive score results to measures of brain atrophy improved ability to predict future conversion from MCI to AD(76). Regional volumes along with CSF biomarkers showed modestly improved ability to predict conversion of MCI to AD over the use of either alone, with combined accuracy of 69%(77). A combination of CSF measurements of tau protein and hippocampal atrophy on MRI was shown to identify from a population of cognitively intact individuals those who are likely to show deterioration in cognitive testing(78). Classification schemes using baseline MRI, PET, and CSF biomarkers have shown improved accuracy in classifying MCI patients from cognitively normal and in predicting conversion from MCI to AD(74, 75). A general principle that appears to be emerging is that amyloid PET may provide a more certain etiologic diagnosis, but that neurodegenerative biomarkers, such as ^{18}F -FDG PET and structural imaging, may better track disease severity and the timing of progression in MCI and perhaps cognitively normal individuals(35). Thus, these methods serve complementary roles.

Future imaging biomarkers and technology

Novel MRI sequences and PET radiotracers have the potential to further improve evaluation of patients with cognitive decline and dementia. These novel MRI sequences and radiotracers are being applied in research settings and have been informative on the pathophysiology of neurodegenerative dementia, but not yet adequately validated for routine clinical use.

Perhaps the most likely MRI sequence to translate to the clinic is Arterial Spin Labeling (ASL), which measures cerebral perfusion. ASL shows hypoperfusion in regions similar to those seen on ^{18}F -FDG PET and with SPECT perfusion agents in AD(79). Furthermore, differences in cerebral perfusion between AD and FTLN on ASL MRI show promise in differential diagnosis(80). Thus, ASL could add information previously evaluated only on PET and SPECT to a routine MRI study, although further standardization of this sequence particularly between MRI scanner vendors will be required. MRI can also detect changes in regional neural activation patterns using Blood Oxygen Level Dependent (BOLD) functional MRI (fMRI), which measures local changes in blood oxygenation caused by alterations in synaptic activity. BOLD fMRI can be used to evaluate brain activity during specific tasks, such as a language task, or while at rest to assess regions with co-varied BOLD signal reflecting brain network functional connectivity. Studies have detected alterations in BOLD signal in demented patients, including decreased activation in the hippocampi on memory tasks on fMRI(81) and disruptions in functional connectivity on resting state fMRI(82). These techniques currently appear more suited to research applications than clinical evaluation at present.

Numerous PET radiotracers have been developed that are applicable to evaluation of neurodegenerative disease. Currently, there is great interest in newly developed radiotracers with potential to detect the pattern of deposition of tau protein, including ^{18}F AV-1451 (formerly T807) and ^{18}F -THK523(10, 83). Tau is the principle component of neurofibrillary tangles, one of the hallmark neuropathologic features of AD, and also forms aggregates in multiple other neurodegenerative diseases, including multiple subtypes of FTLN. Tau aggregates are neurotoxic; the presence of tau aggregates is associated with neurodegeneration. The degree and distribution of neurofibrillary tangle pathology is more closely related to the pattern and severity of clinical symptoms in AD than amyloid(84). The ability to provide information on the spatial distribution and extent of tau deposition make these PET tracers more likely to better track disease severity than a scalar, global measure like CSF tau. PET radiotracers targeting neuroinflammation/microglial activation have also shown promise in studying AD in early studies, showing significant differences between AD and cognitively normal groups and correlation of binding with clinical severity(85).

Recent technologic advancements have allowed construction of combined PET/MRI scanners, which have had limited clinical use to date. These combined scanners have the potential to acquire both MRI and PET data within the time of a single traditional MRI scan, adding diagnostic information without additional time or testing, which can be challenging for patients with dementia. Post-acquisition image coregistration is relatively straightforward for the brain, so combining standard MRI and PET acquisitions on one system adds little diagnostic information. PET/MRI scanners are uniquely capable of simultaneous evaluation of dynamic processes in the brain, particularly using dynamic PET acquisitions with novel radiotracers and functional MRI. These have clear potential for research applications; it remains to be seen whether such information will be clinically useful.

Conclusion

Neuroimaging allows for earlier and more accurate diagnosis and prognosis for neurodegenerative dementia and individuals with cognitive decline. Diagnostic criteria for these conditions are being revised to include imaging biomarker findings, including recent updates for MCI and AD(19). For AD, there is evidence for an ordered sequence of change of imaging biomarkers, with early abnormality on amyloid PET followed by various measures of neurodegeneration quantified on structural MRI and ¹⁸F-FDG PET (28). Increasing efforts to combine biomarker data to further improve diagnostic accuracy must be tested in independent and inclusive samples to prove validity. Selected appropriately, multimodality imaging with MRI and PET has the potential to improve diagnosis and management of patients with neurodegenerative dementia, providing complementary information that may be acquired simultaneously with upcoming PET/MRI scanners. The value of imaging biomarkers will be greatly enhanced with development of disease modifying therapies.

References

1. Fox C, Lafortune L, Boustani M, Dening T, Rait G, Brayne C. Screening for dementia—is it a no brainer? *International journal of clinical practice*. 2013; 67:1076–1080. [PubMed: 23952529]
2. World Alzheimer Report 2011. <http://www.alzco.uk/research/world-report-2011>.
3. Josephs KA. Frontotemporal dementia and related disorders: deciphering the enigma. *Annals of neurology*. 2008; 64:4–14. [PubMed: 18668533]
4. Herholz K. Perfusion SPECT and FDG-PET. *International psychogeriatrics/IPA*. 2011; 23(Suppl 2):S25–31. [PubMed: 21729421]
5. Mosconi L, Tsui WH, Herholz K, et al. Multicenter standardized ¹⁸F-FDG PET diagnosis of mild cognitive impairment, Alzheimer's disease, and other dementias. *Journal of nuclear medicine: official publication, Society of Nuclear Medicine*. 2008; 49:390–398.
6. Panegyres PK, Rogers JM, McCarthy M, Campbell A, Wu J. Fluorodeoxyglucose-Positron Emission Tomography in the differential diagnosis of early-onset dementia: a prospective, community-based study. *BMC Neurology*. 2009; 9:41. [PubMed: 19674446]
7. Mason NS, Mathis CA, Klunk WE. Positron emission tomography radioligands for in vivo imaging of Aβ plaques. *Journal of labelled compounds & radiopharmaceuticals*. 2013; 56:89–95. [PubMed: 24285314]
8. Landau SM, Breault C, Joshi AD, et al. Amyloid-beta imaging with Pittsburgh compound B and florbetapir: comparing radiotracers and quantification methods. *Journal of nuclear medicine: official publication, Society of Nuclear Medicine*. 2013; 54:70–77.
9. Clark CM, Pontecorvo MJ, Beach TG, et al. Cerebral PET with florbetapir compared with neuropathology at autopsy for detection of neuritic amyloid-β plaques: a prospective cohort study. *The Lancet Neurology*. 2012; 11:669–678. [PubMed: 22749065]
10. Chien DT, Bahri S, Szardenings AK, et al. Early clinical PET imaging results with the novel PHF-tau radioligand [F-18]-T807. *Journal of Alzheimer's disease: JAD*. 2013; 34:457–468. [PubMed: 23234879]
11. Herholz K, Salmon E, Perani D, et al. Discrimination between Alzheimer dementia and controls by automated analysis of multicenter FDG PET. *NeuroImage*. 2002; 17:302–316. [PubMed: 12482085]
12. Davatzikos C, Xu F, An Y, Fan Y, Resnick SM. Longitudinal progression of Alzheimer's-like patterns of atrophy in normal older adults: the SPARE-AD index. *Brain: a journal of neurology*. 2009; 132:2026–2035. [PubMed: 19416949]

13. Foster NL, Heidebrink JL, Clark CM, et al. FDG-PET improves accuracy in distinguishing frontotemporal dementia and Alzheimer's disease. *Brain: a journal of neurology*. 2007; 130:2616–2635. [PubMed: 17704526]
14. Rabinovici GD, Rosen HJ, Alkalay A, et al. Amyloid vs FDG-PET in the differential diagnosis of AD and FTLN. *Neurology*. 2011; 77:2034–2042. [PubMed: 22131541]
15. Fjell AM, Walhovd KB, Fennema-Notestine C, et al. One-year brain atrophy evident in healthy aging. *The Journal of neuroscience: the official journal of the Society for Neuroscience*. 2009; 29:15223–15231. [PubMed: 19955375]
16. Nosheny RL, Insel PS, Truran D, et al. Variables associated with hippocampal atrophy rate in normal aging and mild cognitive impairment. *Neurobiology of Aging*. 2014
17. Rowe CC, Ellis KA, Rimajova M, et al. Amyloid imaging results from the Australian Imaging, Biomarkers and Lifestyle (AIBL) study of aging. *Neurobiology of Aging*. 2010; 31:1275–1283. [PubMed: 20472326]
18. Sperling RA, Karlawish J, Johnson KA. Preclinical Alzheimer disease—the challenges ahead. *Nature reviews Neurology*. 2013; 9:54–58.
19. McKhann GM, Knopman DS, Chertkow H, et al. The diagnosis of dementia due to Alzheimer's disease: recommendations from the National Institute on Aging–Alzheimer's Association workgroups on diagnostic guidelines for Alzheimer's disease. *Alzheimer's & dementia: the journal of the Alzheimer's Association*. 2011; 7:263–269.
20. Albert MS, DeKosky ST, Dickson D, et al. The diagnosis of mild cognitive impairment due to Alzheimer's disease: Recommendations from the National Institute on Aging–Alzheimer's Association workgroups on diagnostic guidelines for Alzheimer's disease. *Alzheimer's & Dementia*. 2011; 7:270–279.
21. Sperling RA, Aisen PS, Beckett LA, et al. Toward defining the preclinical stages of Alzheimer's disease: recommendations from the National Institute on Aging–Alzheimer's Association workgroups on diagnostic guidelines for Alzheimer's disease. *Alzheimer's & dementia: the journal of the Alzheimer's Association*. 2011; 7:280–292.
22. Shi F, Liu B, Zhou Y, Yu C, Jiang T. Hippocampal volume and asymmetry in mild cognitive impairment and Alzheimer's disease: Meta-analyses of MRI studies. *Hippocampus*. 2009; 19:1055–1064. [PubMed: 19309039]
23. Yushkevich PA, Pluta JB, Wang H, et al. Automated volumetry and regional thickness analysis of hippocampal subfields and medial temporal cortical structures in mild cognitive impairment. *Human brain mapping*. 2014
24. Da X, Toledo JB, Zee J, et al. Integration and relative value of biomarkers for prediction of MCI to AD progression: Spatial patterns of brain atrophy, cognitive scores, APOE genotype and CSF biomarkers. *NeuroImage Clinical*. 2014; 4:164–173. [PubMed: 24371799]
25. Minoshima S, Giordani B, Berent S, Frey KA, Foster NL, Kuhl DE. Metabolic reduction in the posterior cingulate cortex in very early Alzheimer's disease. *Annals of neurology*. 1997; 42:85–94. [PubMed: 9225689]
26. Kadir A, Almkvist O, Forsberg A, et al. Dynamic changes in PET amyloid and FDG imaging at different stages of Alzheimer's disease. *Neurobiology of Aging*. 2012; 33:198e191–114. [PubMed: 20688420]
27. Dukart J, Mueller K, Villringer A, et al. Relationship between imaging biomarkers, age, progression and symptom severity in Alzheimer's disease. *NeuroImage Clinical*. 2013; 3:84–94. [PubMed: 24179852]
28. Jack CR Jr, Knopman DS, Jagust WJ, et al. Tracking pathophysiological processes in Alzheimer's disease: an updated hypothetical model of dynamic biomarkers. *The Lancet Neurology*. 2013; 12:207–216. [PubMed: 23332364]
29. Drzezga A, Lautenschlager N, Siebner H, et al. Cerebral metabolic changes accompanying conversion of mild cognitive impairment into Alzheimer's disease: a PET follow-up study. *European journal of nuclear medicine and molecular imaging*. 2003; 30:1104–1113. [PubMed: 12764551]

30. Teune LK, Bartels AL, de Jong BM, et al. Typical cerebral metabolic patterns in neurodegenerative brain diseases. *Movement disorders: official journal of the Movement Disorder Society*. 2010; 25:2395–2404. [PubMed: 20669302]
31. Jagust W, Reed B, Mungas D, Ellis W, Decarli C. What does fluorodeoxyglucose PET imaging add to a clinical diagnosis of dementia? *Neurology*. 2007; 69:871–877. [PubMed: 17724289]
32. Laforce R Jr, Buteau JP, Paquet N, Verret L, Houde M, Bouchard RW. The value of PET in mild cognitive impairment, typical and atypical/unclear dementias: A retrospective memory clinic study. *American journal of Alzheimer's disease and other dementias*. 2010; 25:324–332.
33. Vandenberghe R, Adamczuk K, Dupont P, Laere KV, Chetelat G. Amyloid PET in clinical practice: Its place in the multidimensional space of Alzheimer's disease. *NeuroImage Clinical*. 2013; 2:497–511. [PubMed: 24179802]
34. Wolk DA, Price JC, Saxton JA, et al. Amyloid imaging in mild cognitive impairment subtypes. *Annals of neurology*. 2009; 65:557–568. [PubMed: 19475670]
35. Jack CR Jr, Wiste HJ, Vemuri P, et al. Brain beta-amyloid measures and magnetic resonance imaging atrophy both predict time-to-progression from mild cognitive impairment to Alzheimer's disease. *Brain: a journal of neurology*. 2010; 133:3336–3348. [PubMed: 20935035]
36. Koedam EL, Lauffer V, van der Vlies AE, van der Flier WM, Scheltens P, Pijnenburg YA. Early- versus late-onset Alzheimer's disease: more than age alone. *Journal of Alzheimer's disease: JAD*. 2010; 19:1401–1408. [PubMed: 20061618]
37. Wolk DA. Amyloid imaging in atypical presentations of Alzheimer's disease. *Current neurology and neuroscience reports*. 2013; 13:412. [PubMed: 24136459]
38. Migliaccio R, Agosta F, Rascovsky K, et al. Clinical syndromes associated with posterior atrophy: early age at onset AD spectrum. *Neurology*. 2009; 73:1571–1578. [PubMed: 19901249]
39. Wolk DA, Price JC, Madeira C, et al. Amyloid imaging in dementias with atypical presentation. *Alzheimer's & dementia: the journal of the Alzheimer's Association*. 2012; 8:389–398.
40. Pereira JM, Williams GB, Acosta-Cabronero J, et al. Atrophy patterns in histologic vs clinical groupings of frontotemporal lobar degeneration. *Neurology*. 2009; 72:1653–1660. [PubMed: 19433738]
41. Lindberg O, Ostberg P, Zandbelt BB, et al. Cortical morphometric subclassification of frontotemporal lobar degeneration. *AJNR American journal of neuroradiology*. 2009; 30:1233–1239. [PubMed: 19346314]
42. Rohrer JD, Geser F, Zhou J, et al. TDP-43 subtypes are associated with distinct atrophy patterns in frontotemporal dementia. *Neurology*. 2010; 75:2204–2211. [PubMed: 21172843]
43. Jeong Y, Cho SS, Park JM, et al. 18F-FDG PET findings in frontotemporal dementia: an SPM analysis of 29 patients. *Journal of nuclear medicine: official publication, Society of Nuclear Medicine*. 2005; 46:233–239.
44. Nestor PJ, Fryer TD, Hodges JR. Declarative memory impairments in Alzheimer's disease and semantic dementia. *NeuroImage*. 2006; 30:1010–1020. [PubMed: 16300967]
45. Poljansky S, Ibach B, Hirschberger B, et al. A visual [18F]FDG-PET rating scale for the differential diagnosis of frontotemporal lobar degeneration. *European archives of psychiatry and clinical neuroscience*. 2011; 261:433–446. [PubMed: 21207049]
46. Villemagne VL, Ong K, Mulligan RS, et al. Amyloid imaging with (18)F-florbetaben in Alzheimer disease and other dementias. *Journal of nuclear medicine: official publication, Society of Nuclear Medicine*. 2011; 52:1210–1217.
47. Rabinovici GD, Furst AJ, O'Neil JP, et al. 11C-PIB PET imaging in Alzheimer disease and frontotemporal lobar degeneration. *Neurology*. 2007; 68:1205–1212. [PubMed: 17420404]
48. Kitagaki H, Hirono N, Ishii K, Mori E. Corticobasal degeneration: evaluation of cortical atrophy by means of hemispheric surface display generated with MR images. *Radiology*. 2000; 216:31–38. [PubMed: 10887225]
49. Wadia PM, Lang AE. The many faces of corticobasal degeneration. *Parkinsonism & related disorders*. 2007; 13(Suppl 3):S336–340. [PubMed: 18267261]
50. McKeith IG. Consensus guidelines for the clinical and pathologic diagnosis of dementia with Lewy bodies (DLB): report of the Consortium on DLB International Workshop. *Journal of Alzheimer's disease: JAD*. 2006; 9:417–423.

51. Edison P, Rowe CC, Rinne JO, et al. Amyloid load in Parkinson's disease dementia and Lewy body dementia measured with [11C]PIB positron emission tomography. *Journal of neurology, neurosurgery, and psychiatry*. 2008; 79:1331–1338.
52. Whitwell JL, Weigand SD, Shiung MM, et al. Focal atrophy in dementia with Lewy bodies on MRI: a distinct pattern from Alzheimer's disease. *Brain: a journal of neurology*. 2007; 130:708–719. [PubMed: 17267521]
53. Gilman S, Koeppe RA, Little R, et al. Differentiation of Alzheimer's disease from dementia with Lewy bodies utilizing positron emission tomography with [18F]fluorodeoxyglucose and neuropsychological testing. *Experimental neurology*. 2005; 191(Suppl 1):S95–S103. [PubMed: 15629765]
54. Papanthasiou ND, Boutsiadis A, Dickson J, Bomanji JB. Diagnostic accuracy of [I-123]-FP-CIT (DaTSCAN) in dementia with Lewy bodies: a meta-analysis of published studies. *Parkinsonism & related disorders*. 2012; 18:225–229. [PubMed: 21975260]
55. Du AT, Schuff N, Kramer JH, et al. Different regional patterns of cortical thinning in Alzheimer's disease and frontotemporal dementia. *Brain: a journal of neurology*. 2007; 130:1159–1166. [PubMed: 17353226]
56. Rohrer JD, Warren JD, Modat M, et al. Patterns of cortical thinning in the language variants of frontotemporal lobar degeneration. *Neurology*. 2009; 72:1562–1569. [PubMed: 19414722]
57. Minoshima S, Foster NL, Sima AA, Frey KA, Albin RL, Kuhl DE. Alzheimer's disease versus dementia with Lewy bodies: cerebral metabolic distinction with autopsy confirmation. *Annals of neurology*. 2001; 50:358–365. [PubMed: 11558792]
58. Benson DF, Kuhl DE, Hawkins RA, Phelps ME, Cummings JL, Tsai SY. The fluorodeoxyglucose 18F scan in Alzheimer's disease and multi-infarct dementia. *Archives of neurology*. 1983; 40:711–714. [PubMed: 6605139]
59. Tripathi M, Damle N, Kushwaha S, et al. Differential diagnosis of neurodegenerative dementias using metabolic phenotypes on F-18 FDG PET/CT. *The neuroradiology journal*. 2014; 27:13–21. [PubMed: 24571830]
60. Perani D, Schillaci O, Padovani A, et al. A survey of FDG- and amyloid-PET imaging in dementia and GRADE analysis. *BioMed research international*. 2014; 2014:785039. [PubMed: 24772437]
61. Matias-Guiu JA, Cabrera-Martin MN, Garcia-Ramos R, et al. Evaluation of the new consensus criteria for the diagnosis of primary progressive aphasia using fluorodeoxyglucose positron emission tomography. *Dementia and geriatric cognitive disorders*. 2014; 38:147–152. [PubMed: 24732287]
62. Prins ND, van der Flier WM, Brashear HR, et al. Predictors of progression from mild cognitive impairment to dementia in the placebo-arm of a clinical trial population. *Journal of Alzheimer's disease: JAD*. 2013; 36:79–85. [PubMed: 23563246]
63. Prestia A, Caroli A, Herholz K, et al. Diagnostic accuracy of markers for prodromal Alzheimer's disease in independent clinical series. *Alzheimer's & dementia: the journal of the Alzheimer's Association*. 2013; 9:677–686.
64. Jack CR Jr, Petersen RC, Xu YC, et al. Prediction of AD with MRI-based hippocampal volume in mild cognitive impairment. *Neurology*. 1999; 52:1397–1403. [PubMed: 10227624]
65. Jack CR Jr, Shiung MM, Weigand SD, et al. Brain atrophy rates predict subsequent clinical conversion in normal elderly and amnesic MCI. *Neurology*. 2005; 65:1227–1231. [PubMed: 16247049]
66. Nestor SM, Rupsingh R, Borrie M, et al. Ventricular enlargement as a possible measure of Alzheimer's disease progression validated using the Alzheimer's disease neuroimaging initiative database. *Brain: a journal of neurology*. 2008; 131:2443–2454. [PubMed: 18669512]
67. Josephs KA Jr, Whitwell JL, Weigand SD, et al. Predicting functional decline in behavioural variant frontotemporal dementia. *Brain: a journal of neurology*. 2011; 134:432–448. [PubMed: 21252111]
68. Nedelska Z, Ferman TJ, Boeve BF, et al. Pattern of brain atrophy rates in autopsy-confirmed dementia with Lewy bodies. *Neurobiology of Aging*. 2014

69. Fujishiro H, Iseki E, Kasanuki K, et al. A follow up study of non-demented patients with primary visual cortical hypometabolism: prodromal dementia with Lewy bodies. *Journal of the neurological sciences*. 2013; 334:48–54. [PubMed: 23927939]
70. Jacova C, Hsiung GY, Tawankanjanachot I, et al. Anterior brain glucose hypometabolism predates dementia in progranulin mutation carriers. *Neurology*. 2013; 81:1322–1331. [PubMed: 24005336]
71. Lowe VJ, Weigand SD, Senjem ML, et al. Association of hypometabolism and amyloid levels in aging, normal subjects. *Neurology*. 2014; 82:1959–1967. [PubMed: 24793183]
72. Rowe CC, Bourgeat P, Ellis KA, et al. Predicting Alzheimer disease with beta-amyloid imaging: results from the Australian imaging, biomarkers, and lifestyle study of ageing. *Annals of neurology*. 2013; 74:905–913. [PubMed: 24448836]
73. Roe CM, Fagan AM, Grant EA, et al. Amyloid imaging and CSF biomarkers in predicting cognitive impairment up to 7.5 years later. *Neurology*. 2013; 80:1784–1791. [PubMed: 23576620]
74. Shaffer JL, Petrella JR, Sheldon FC, et al. Predicting cognitive decline in subjects at risk for Alzheimer disease by using combined cerebrospinal fluid, MR imaging, and PET biomarkers. *Radiology*. 2013; 266:583–591. [PubMed: 23232293]
75. Zhang D, Shen D. Multi-modal multi-task learning for joint prediction of multiple regression and classification variables in Alzheimer’s disease. *NeuroImage*. 2012; 59:895–907. [PubMed: 21992749]
76. Gross AL, Manly JJ, Pa J, et al. Cortical signatures of cognition and their relationship to Alzheimer’s disease. *Brain imaging and behavior*. 2012; 6:584–598. [PubMed: 22718430]
77. Westman E, Muehlboeck JS, Simmons A. Combining MRI and CSF measures for classification of Alzheimer’s disease and prediction of mild cognitive impairment conversion. *NeuroImage*. 2012; 62:229–238. [PubMed: 22580170]
78. Nettiksimmons J, Harvey D, Brewer J, et al. Subtypes based on cerebrospinal fluid and magnetic resonance imaging markers in normal elderly predict cognitive decline. *Neurobiology of Aging*. 2010; 31:1419–1428. [PubMed: 20542598]
79. Johnson NA, Jahng GH, Weiner MW, et al. Pattern of cerebral hypoperfusion in Alzheimer disease and mild cognitive impairment measured with arterial spin-labeling MR imaging: initial experience. *Radiology*. 2005; 234:851–859. [PubMed: 15734937]
80. Hu WT, Wang Z, Lee VM, Trojanowski JQ, Detre JA, Grossman M. Distinct cerebral perfusion patterns in FTLN and AD. *Neurology*. 2010; 75:881–888. [PubMed: 20819999]
81. Celone KA, Calhoun VD, Dickerson BC, et al. Alterations in memory networks in mild cognitive impairment and Alzheimer’s disease: an independent component analysis. *The Journal of neuroscience: the official journal of the Society for Neuroscience*. 2006; 26:10222–10231. [PubMed: 17021177]
82. Thomas JB, Brier MR, Bateman RJ, et al. Functional Connectivity in Autosomal Dominant and Late-Onset Alzheimer Disease. *JAMA neurology*. 2014
83. Fodero-Tavoletti MT, Okamura N, Furumoto S, et al. 18F-THK523: a novel in vivo tau imaging ligand for Alzheimer’s disease. *Brain: a journal of neurology*. 2011; 134:1089–1100. [PubMed: 21436112]
84. Arriagada PV, Growdon JH, Hedley-Whyte ET, Hyman BT. Neurofibrillary tangles but not senile plaques parallel duration and severity of Alzheimer’s disease. *Neurology*. 1992; 42:631–639. [PubMed: 1549228]
85. Kreisl WC, Lyoo CH, McGwier M, et al. In vivo radioligand binding to translocator protein correlates with severity of Alzheimer’s disease. *Brain: a journal of neurology*. 2013; 136:2228–2238. [PubMed: 23775979]

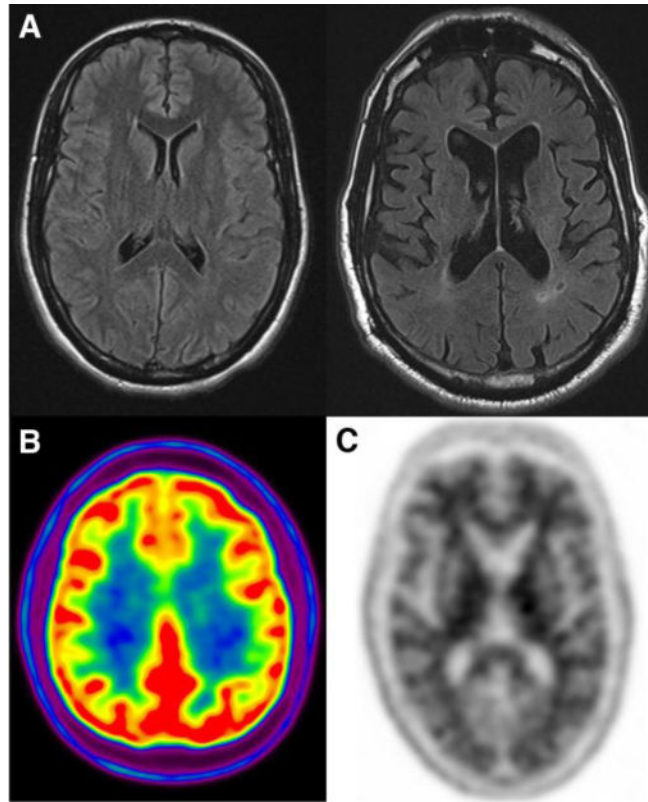


Figure 1. Imaging of cognitively normal individuals. (A) Axial FLAIR shows normal appearance of the brain on MRI in a young adult in third decade and typical appearance of a brain MRI in the eighth decade, showing mild atrophy and mild white matter hyperintensities. (B) Normal ^{18}F -FDG PET shows high uptake in gray matter structures. (C) Normal amyloid PET scan with the radiotracer ^{18}F -florbetapir shows typical white matter uptake but no evidence of elevated cortical binding.

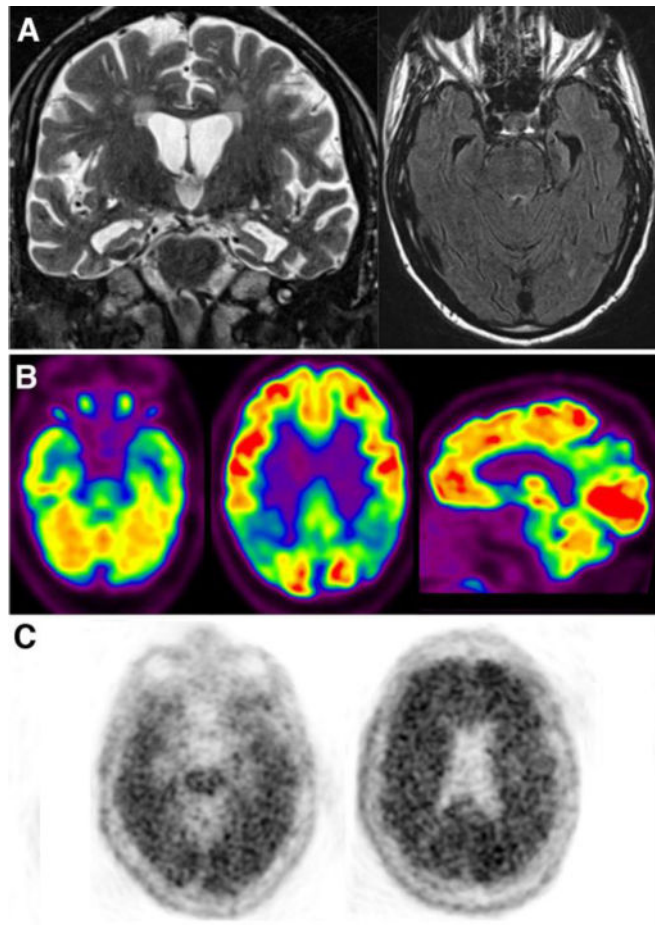


Figure 2. Neuroimaging in AD. (A) Coronal T2 and axial FLAIR MRI images show marked medial temporal lobe atrophy involving hippocampus and subjacent entorhinal cortex, out of proportion to global volume loss. (B) Axial and sagittal images from an ^{18}F -FDG PET shows typical lateral temporoparietal, posterior cingulate, and medial temporal lobe hypometabolism. Milder frontal hypometabolism is present, also common. (C) Axial images from a positive amyloid PET scan with ^{18}F -florbetapir showing diffuse cortical activity with loss of the distinction between gray and white matter.

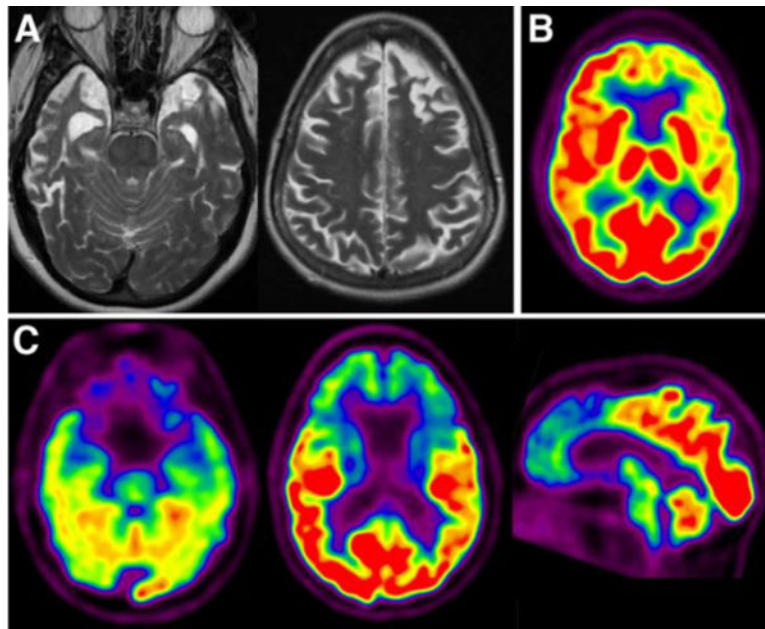


Figure 3. Neuroimaging in FTLD. (A) Axial T2 images from two patients show two characteristic patterns of FTLD: anterior temporal and frontal atrophy. Both show asymmetry and knife blade appearance of the gyri. ^{18}F -FDG PET shows two typical patterns: left frontotemporoparietal hypometabolism (B, axial) versus frontal-predominant (C, axial and sagittal).

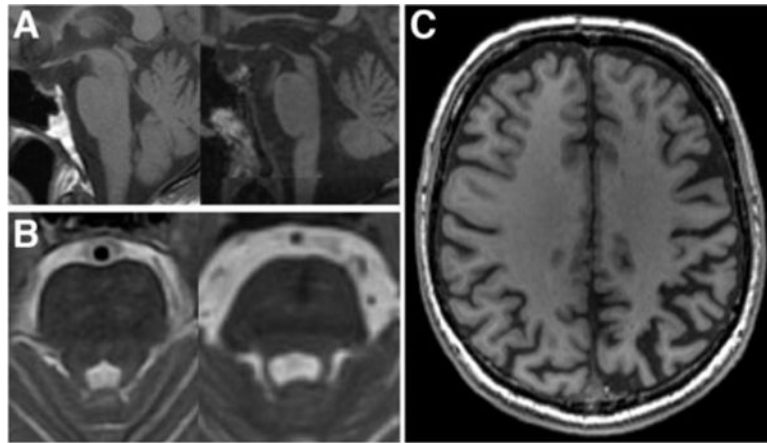


Figure 4.

MRI appearance of PSP and CBD subtypes of FTLD. Normal sagittal T1 and axial T2 images centered on the brainstem, shown for comparison on the left in parts A and B. In PSP (A), there is severe midbrain atrophy with ‘hummingbird’ appearance of the brainstem; note the shortened anteroposterior dimension of the midbrain and concave superior margin. (B) Superior cerebellar peduncle atrophy in PSP. (C) Axial T1 image shows asymmetric left frontoparietal atrophy in CBD.

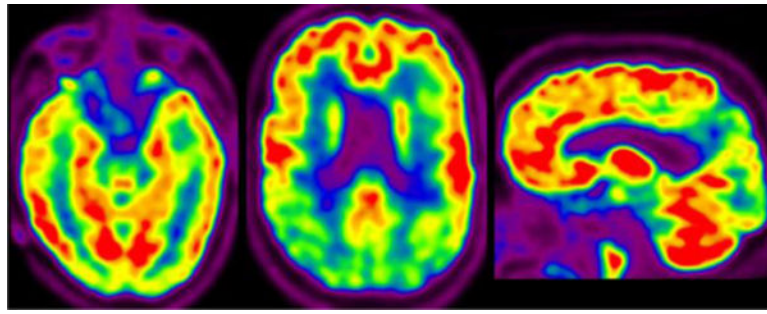


Figure 5. ^{18}F -FDG PET in DLB. Axial images through the levels of the temporal lobes and lateral ventricles and parasagittal image show occipital and posterior temporoparietal hypometabolism. Note sparing of the posterior cingulate cortex and medial temporal lobes.

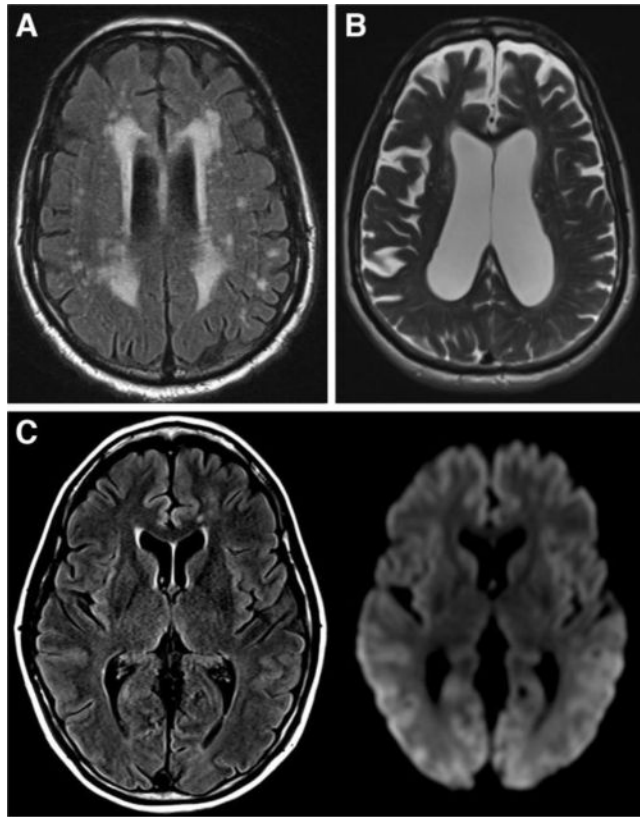


Figure 6. MRI appearance of selected secondary causes of dementia. (A) Marked small vessel ischemic changes manifested by confluent periventricular hyperintensity and subcortical lesions on axial FLAIR. (B) Axial T2 shows enlarged ventricles in a patient with normal pressure hydrocephalus, out of proportion to the degree of diffuse atrophy. (C) Axial FLAIR and diffusion weighted images in a patient with CJD show diffuse cortical and asymmetric deep gray matter signal abnormality most evident on diffusion imaging.